PHYSICAL REVIEW B **81**, 180402(R) (2010)

Effective quantum dimer model for the kagome Heisenberg antiferromagnet: Nearby quantum critical point and hidden degeneracy

Didier Poilblanc, Matthieu Mambrini, and David Schwandt
Laboratoire de Physique Théorique, CNRS and Université de Toulouse, F-31062 Toulouse, France
(Received 7 April 2010; published 13 May 2010)

The low-energy singlet dynamics of the quantum Heisenberg antiferromagnet on the kagome lattice is described by a quantitative quantum dimer model. Using advanced numerical tools, the latter is shown to exhibit valence-bond crystal (VBC) order with a large 36-site unit cell and hidden degeneracy between even odd parities. Evidences are given that this ground state lies in the vicinity of a $\mathbb{Z}_2$ dimer-liquid region separated by a quantum critical point (QCP). Implications regarding numerical analysis and experiments are discussed.

DOI: 10.1103/PhysRevB.81.180402 PACS number(s): 75.10.Jm, 64.70.Tg, 67.80.kb, 74.20.Mn

I. INTRODUCTION

The kagome lattice, a two-dimensional corner-sharing array of triangles shown in Fig. 1(a), is believed to be one of the most frustrated lattices leading to finite entropy in the ground state (GS) of the classical Heisenberg model.[1] Hence, the quantum $S=1/2$ Heisenberg antiferromagnet (QHAF) on the kagome lattice is often considered as the paradigm of quantum frustrated magnetism,[2] where, in contrast to conventional broken-symmetry phases of spin systems (as, e.g., magnetic phases), exotic *quantum liquids or crystals* could be realized. Among the latter, the algebraic (gapless) spin liquid is one of the most intriguing candidate.[3]

The herbertsmithite[4] compound is one of the few experimental realizations of the $S=1/2$ kagome QHAF. The absence of magnetic ordering[5] down to temperatures much smaller than the typical energy scale of the exchange coupling J suggests that, indeed, intrinsic properties of the kagome QHAF can be observed, even though NMR and ESR reveal a small fraction of nonmagnetic impurities[6] and small Dzyaloshinsky-Moriya anisotropy.[7] So far, the nature of the nonmagnetic phase is unknown and confrontation to new theoretical ideas have become necessary. Alternatively, ultracold atoms loaded on an optical lattice with tunable interactions might enable to also explore the physics of extended kagome QHAF.[8]

The QHAF on the kagome lattice has been addressed theoretically by Lanczos exact diagonalization (LED) of small clusters.[9,10] Despite the fact that the accessible cluster sizes remain very small, these data are consistent with a finite spin gap and an exponential number of singlets within the gap, in agreement with a recent density-matrix renormalization-group study.[11] In addition, an analysis of the four-spin correlations pointed toward a *short-range* dimer-liquid phase.[12] Alternatively, a large-N approach[13] and various mappings to low-energy effective Hamiltonians within the singlet subspace[14–16] have suggested the formation of translation symmetry breaking valence-bond crystals (VBC). Recently, recent series expansions around the dimer limit[17] showed that a 36-site VBC unit cell is preferred [see Fig. 1(a)]. In this context, the interpretation of the LED low-energy singlet spectrum remains problematic.[18]

In this Rapid Communication, we use a quantitative dimer-projected effective model to describe the low-energy singlet subspace of the kagome QHAF. This is based on a controlled loop expansion[19] along the lines initiated by Rokhsar and Kivelson (RK) (Ref. 20) in the context of high-temperature superconductivity and by Zeng and Elser[21] (ZE) for the kagome lattice. LED of the effective model enable to reach unprecedented sizes of periodic clusters which can accommodate a finite number of candidate VBC unit cells. The major results are (i) the numerical evidence of VBC order with a large 36-site unit cell and a hidden degeneracy, (ii) the vicinity of a $\mathbb{Z}_2$ dimer-liquid region separated by a quantum critical point (QCP). Such results transposed to the original QHAF could explain some of its former puzzling numerical findings.

II. MODEL

The method consists in projecting the QHAF, $\mathcal{H}=J\Sigma_{\langle i,j\rangle}\mathbf{S}_i\cdot\mathbf{S}_j$, i and j being nearest-neighbor (NN) lattice

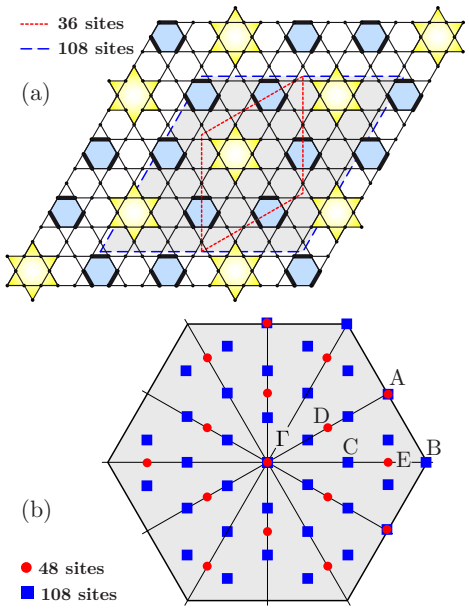

FIG. 1. (Color online) (a) Sketch of the 36-site VBC on the kagome lattice showing "perfect hexagons" and (yellow) star resonances. Its unit cell is delimited by dashed (red) lines. The extension of the 108-site cluster (which fits exactly three 36-site cells) is (lightly) shaded and delimited by long-dashed (blue) lines. Hard-core dimers (formed by two neighboring spin-$\frac{1}{2}$) are located on the bonds (only shown on the shaded hexagons). (b) First Brillouin zone and available momenta (labeling consistent with Ref. 18).

TABLE I. Quantum numbers of the GS multiplet for VBC with $\mathcal{N}$-site cells ($\mathcal{N}=3\times m\times m$ or $\mathcal{N}=3\times n\sqrt{3}\times n\sqrt{3}$) and degeneracy $\mathcal{N}/3$. The letters refer to the momenta of Fig. 1. Invariance under $2\pi/3$ rotations ($r_3=+$) and parity under inversion ($r_2=\pm$) and/or reflection about the momentum direction (σ) are denoted as (r_3,r_2,σ) consistently with Ref. 18. $\sigma=\pm$ corresponds to even or odd GS and "×" means "symmetry not relevant." The $\mathbb{Z}_2$ dimer-liquid (last line) GS in TS^* is degenerate with the other TS GS (Ref. 27).

VBC	Γ	A	B	C	D	E
$\mathcal{N}=12$	$(+,+,\pm)$	$(\times,+,\pm)$				
$\mathcal{N}=36$	$(+,+,\pm)$	$(\times,+,\pm)$	$(+,\times,\pm)$	$(\times,\times,\pm)$		
$\mathcal{N}=48$	$(+,+,\pm)$	$(\times,+,\pm)$			$(\times,\times,\pm)$	$(\times,\times,\pm)$
$\mathbb{Z}_2$	$(+,+,+)$					

sites, into the manifold formed by NN VB coverings, an approximation shown to be excellent for the kagome lattice.[21–23] A transformation is then performed that turns the nonorthogonal VB basis into an orthogonal quantum dimer basis. Overlaps between NN and VB states can be written[24] (up to a sign) as α^{N-2n_l}, where N is the system size, n_l the number of loops obtained by superimposing the two configurations, and $\alpha=1/\sqrt{2}$. This enables a systematic expansion in powers of α involving at order α^{2p} ($p\geq 2$) loops of sizes up to $\mathcal{L}=2p+2$ (Refs. 19 and 25) leading to a generalized quantum dimer model (QDM), which restricting to loops encircling only single hexagons, reads

$\mathcal{H}_{\text{eff}} = -J_6 - J_8 (+ +) - J_{10} (+ +) - J_{12}$ (1)

$+V_6 + V_8 (+ +) + V_{10} (+ +) + V_{12}$, (2)

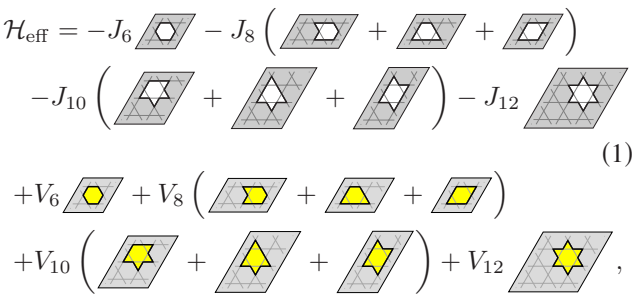

where a sum over all the hexagons of the lattice of Fig. 1(a) is implicit. Kinetic terms in Eq. (1) promote cyclic permutations of the dimers around the loops and diagonal terms in Eq. (2) count the numbers of "flippable" loops. Here we use the approximate values (14th order), $V_6=0.2$, $V_8=0.032$, $V_{10}=V_{12}=0$, $J_6=-0.8$, $J_8=0.251$, $J_{10}=-0.063$, and $J_{12}=0$ (in units of J). Note that the kinetic processes $J_{\mathcal{L}}$ are quite close to ZE (Ref. 21) initial lowest-order estimates, $J_6=-3/4$, $J_8=1/4$, and $J_{10}=-1/16$, a good sign of convergence of the expansion. Very importantly, we also include here the potential $V_{\mathcal{L}}$ terms which appear in our expansion scheme only at order $2(\mathcal{L}-2)$ but play a major role. Note that an exact resummation of the weights of Eqs. (1) and (2) up to all orders can be carried out (leading to tiny deviations) and that the "star" amplitudes J_{12} and V_{12} vanish at all orders.[19]

III. SYMMETRY ANALYSIS

Although the generalized QDM [Eq. (1)] bears a sign problem, it can be addressed by LED of periodic $3\times L^2$ clusters which possess all the infinite lattice symmetries and L^2 unit cells. We shall consider $L=4$ and $L=6$ corresponding to the 48-site and 108-site clusters [see Fig. 1(a)], and use all available lattice symmetries [see available momenta in Fig. 1(b)] to block diagonalize the Hamiltonian in its irreducible representations (IR).[26] We further make use of a topological symmetry which splits the Hilbert space into four topological sectors (TS).[27]

An analysis of the low-energy spectrum and a careful inspection of its quantum numbers provide invaluable informations on the nature of the GS. For a VBC breaking discrete lattice symmetries, a multiplet structure is expected giving rise in the thermodynamic limit to a degenerate GS separated by a gap from the rest of the spectrum. We list in Table I the quantum numbers of the GS multiplet for the most popular VBC in the literature.

IV. QUANTUM CRITICAL POINT

The QDM with only kinetic processes of equal amplitudes, $J_6=J_8=J_{10}=J_{12}(=1/4)$ provides an exactly solvable model[28] $\mathcal{H}_{\text{RK}}$ with a gapped $\mathbb{Z}_2$ dimer-liquid GS with short-range dimer correlations, similarly to the RK point of the triangular QDM.[29] Interestingly, the first excitations (of energy J) correspond to pairs of (localized) topological vortices (visons). It is tempting to construct a simple interpolation $\mathcal{H}(\lambda)=\lambda\mathcal{H}_{\text{eff}}+(1-\lambda)\mathcal{H}_{\text{RK}}$ between this known limit and the effective model Eqs. (1) and (2). Its low-energy spectrum on the 48-site and 108-site clusters is shown as a function of λ in Figs. 2(a) and 2(b), respectively. In the 48-site cluster, a high density of low-energy levels accumulate just above the GS at $\lambda\sim 1$. This strongly suggests the vicinity of a QCP characterized by vortex (vison) condensation as in the triangular QDM.[30] A closer look around $\lambda=1$ on the larger cluster reveals a sudden collapse of the low-energy excitations, clearly before $\lambda=1$. Remarkably, as shown in Fig. 2(c), this collapse coincides exactly with a very sharp peak of the second derivative of GS energy[31] $\chi_\lambda=-\partial^2(E_N^{\text{GS}}/N)/\partial\lambda^2$, enabling to locate the QCP at $\lambda_{\text{QCP}}\sim 0.9357$. Note that the even-parity ($\sigma=+$) multivison excitations at momenta K_{A} and K_{B} merge with the GS precisely at λ_{QCP} (see below).

V. VBC AND HIDDEN DEGENERACY

Next, to identify the ordered phase for $\lambda>\lambda_{\text{QCP}}$ we add a finite star resonance amplitude J_{12} to H_{eff}. As seen in Figs. 3 and 4, this term has a crucial role. In fact, $J_{12}=0$ is highly singular with a (almost exact) degeneracy between odd ($\sigma=-$) and even ($\sigma=+$) states. Physically, we believe it is

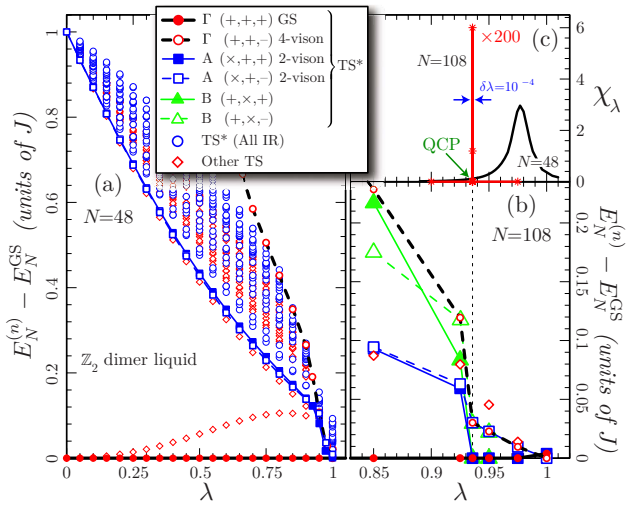

FIG. 2. (Color online) (a) Complete low-energy excitation spectrum of the 48-site cluster as a function of the parameter λ (see text). The lowest 25 levels are displayed in each TS (see Ref. 27) using different symbols/colors. The 2-vison (blue lines) and 4-vison (dashed black line) gaps vanish around $\lambda=1$. (b) Close up around $\lambda=1$ showing the excitation energy of the lowest level of the most relevant IR (see Table I) of the 108-site cluster: a QCP is identified from (i) a collapse of these excitations (b) and (ii) a very sharp peak in χ_λ (c) (data for $N=108$ divided by 200 to fit the scale). Note the transition is far more abrupt for $N=108$ than for $N=48$ (c).

related to the hidden Ising variables (introduced in Ref. 17) associated to the resonance parities of stars [see Fig. 1(a) for the 36-site VBC]. Incidentally, it is remarkable that our effective model picks up such a feature via a vanishing effective J_{12}. For finite but still very small J_{12}, this degeneracy is lifted (favoring a "ferromagnetic" Ising configuration) allowing to characterize any candidate VBC (which should exist with both parity) from its lowest energy states.

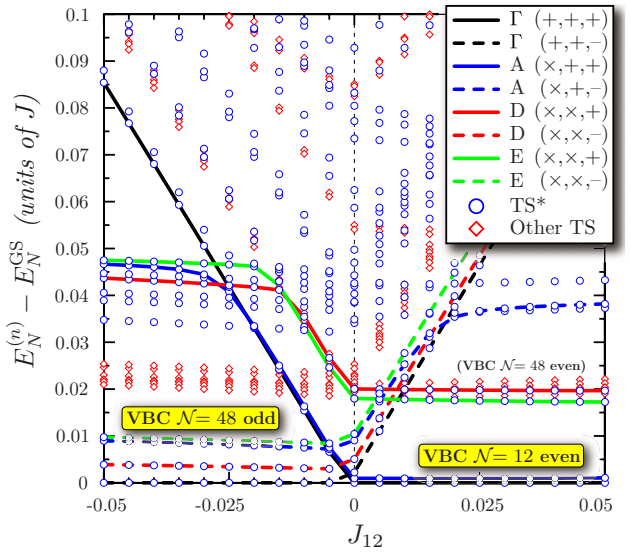

FIG. 3. (Color online) Complete low-energy excitation spectrum of the 48-site cluster as a function of J_{12}. The lowest 25 levels are displayed in each TS [same symbols as Fig. 2(a)]. The quantum numbers of the four lowest-energy states for $J_{12}<0$ and $J_{12}>0$ are provided using different line types.

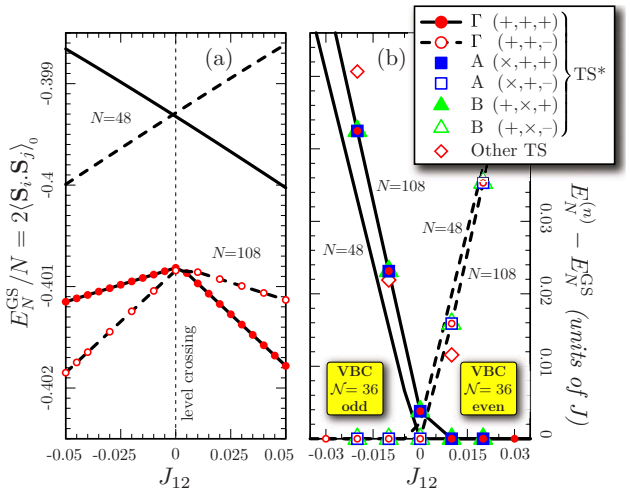

FIG. 4. (Color online) (a) GS energies per site versus J_{12} for $K=K_\Gamma$ and $\sigma=\pm$. The minimum defines the absolute GS energy E_N^{GS}/N. Data for 48 sites (lines) and 108 sites (circles) are shown. An energy shift and scale transformation $E_N \to \frac{3}{4}(E_N - N/2)$ allow a direct comparison with twice the bond energy of the QHAF. (b) Same as Fig. 2(b) but as a function of J_{12} and compared to the $N=48$ excitation at the Γ point (full lines). Note the splittings between Γ, A, and B levels of a few 10^{-8} J are invisible at this scale.

For the 48-site cluster, a close inspection of the associated quantum numbers and a comparison with Table I suggest a VBC with a 48-site (12-site) unit cell for $J_{12}<0$ ($J_{12}>0$). For $J_{12}>0$ slow fluctuations toward the pattern of a $\mathcal{N}=48$ VBC are signaled by the presence of intermediate midgap states. Note that the lowest-energy excitations in the other TS (red lozenges) which barely depend on J_{12} set roughly the (very small) VBC gap scale. Also, the high density of levels within a small energy window of ~0.1 J above the GS is reminiscent of the singlet sector of the QHAF.[18]

A similar analysis on the larger 108-site cluster[26] provides definite evidence in favor of the 36-site (degenerate) VBC schematically depicted in Fig. 1(a), for $\lambda>\lambda_{QCP}$. First, Fig. 4(a) shows a kink at $J_{12}=0$ of the GS energy *per site*, coinciding with the crossing of two GS of opposite parity and leading to almost the same slope discontinuity as for $N=48$ (size effects are small). As for $N=48$, this, in fact, corresponds to the level crossings of two *groups of quasidegenerate* GS with opposite parities as shown in Fig. 4(b). We note an extremely fast decrease with N of the gaps between the A and Γ quasidegenerate GS common to both clusters (a few 10^{-3} J for $N=48$ to less than 10^{-7} J for $N=108$). Furthermore, the fact that a state with momentum K_B (not allowed for $N=48$) belongs to these two groups of quasidegenerate GS definitely points toward a $\mathcal{N}=36$ unit cell[32] (which does not fit $N=48$). This is further supported by the values of the average number $N_\mathcal{L}$ of flippable length-$\mathcal{L}$ loops compared in Table II to their values in VBC proposed in the literature.

In summary, we introduced a generalized QDM to describe the low-energy physics of the QHAF on the kagome lattice. In contrast to the latter, its ground-state properties can be addressed by numerical simulations with unprecedented accuracy for a frustrated quantum magnet. In particular, we provide evidence of (i) a 36-site VBC order (with hidden

TABLE II. Average number $N_{\mathcal{L}}$ of flippable length-$\mathcal{L}$ loops normalized to the total number N_H of hexagons. The last three lines correspond to the "frozen" limit of VBC and to the $\mathbb{Z}_2$ dimer liquid.

Ground states	N_6/N_H	N_8/N_H	N_{10}/N_H	N_{12}/N_H
$N=108$; $J_{12}=0.01$	0.154	0.274	0.491	0.081
$N=108$; $J_{12}=-0.01$	0.153	0.275	0.492	0.080
$3\times2\times2$ [a]	0	0.75	0	0.25
$3\times2\sqrt{3}\times2\sqrt{3}$ [b]	0.167	0.25	0.5	0.083
$\mathbb{Z}_2$ dimer liquid[c]	1/32	15/32	15/32	1/32

[a]Reference 14.
[b]References 13, 15, and 17.
[c]Reference 28.

degeneracy), in agreement with recent series expansion[17] and (ii) the vicinity of a QCP toward a topological $\mathbb{Z}_2$ dimer liquid (cf. schematic phase diagram in Fig. 3 of Ref. 19). Interestingly, a double Chern-Simons field theory[33] also describes such a quantum critical point. The above remarkable features of the generalized QDM transposed to the QHAF would resolve mysteries of the (small cluster) QHAF spectrum such as low-energy singlets carrying unexpected quantum numbers[18] and exceptional sensitivity to small perturbations.[34] Experimentally, kagome spin-1/2 systems generically contain small amounts of lattice and/or spin anisotropies[7] or even longer-range exchange interactions and the proximity to a QCP should render the experimental systems very sensitive to them. However, if under some conditions (pressure, chemical substitution, …) low-temperature spin-induced VBC order establishes, it could be revealed via small lattice modulations mediated by some magnetoelastic coupling. Lastly, we note that the above-mentioned perturbations as well as magnetic excitations[35] can be included in our scheme.

ACKNOWLEDGMENTS

We acknowledge support from the French National Research Agency (ANR) and IDRIS (Orsay, France). D.P. thanks G. Misguich and A. Ralko for discussions.

[1] J. T. Chalker, P. C. W. Holdsworth, and E. F. Shender, Phys. Rev. Lett. **68**, 855 (1992).
[2] For review see, e.g., G. Misguich and C. Lhuillier, in *Frustrated Spin Systems*, Chap. 5, edited by H. T. Diep (World-Scientific, Singapore, 2005), p. 229–306.
[3] M. Hermele, Y. Ran, P. A. Lee, and X.-G. Wen, Phys. Rev. B **77**, 224413 (2008).
[4] M. Shores, E. Nytko, B. Bartlett, and D. Nocera, J. Am. Chem. Soc. **127**, 13462 (2005).
[5] P. Mendels, F. Bert, M. A. de Vries, A. Olariu, A. Harrison, F. Duc, J. C. Trombe, J. Lord, A. Amato, and C. Baines, Phys. Rev. Lett. **98**, 077204 (2007).
[6] A. Olariu, P. Mendels, F. Bert, F. Duc, J. C. Trombe, M. A. de Vries, and A. Harrison, Phys. Rev. Lett. **100**, 087202 (2008).
[7] A. Zorko, S. Nellutla, J. van Tol, L. C. Brunel, F. Bert, F. Duc, J. C. Trombe, M. A. de Vries, A. Harrison, and P. Mendels, Phys. Rev. Lett. **101**, 026405 (2008).
[8] J. Ruostekoski, Phys. Rev. Lett. **103**, 080406 (2009).
[9] P. Lecheminant, B. Bernu, C. Lhuillier, L. Pierre, and P. Sindzingre, Phys. Rev. B **56**, 2521 (1997).
[10] P. Sindzingre, G. Misguich, C. Lhuillier, B. Bernu, L. Pierre, C. Waldtmann, and H. U. Everts, Phys. Rev. Lett. **84**, 2953 (2000).
[11] H. C. Jiang, Z. Y. Weng, and D. N. Sheng, Phys. Rev. Lett. **101**, 117203 (2008).
[12] P. W. Leung and Veit Elser, Phys. Rev. B **47**, 5459 (1993).
[13] J. B. Marston and C. Zeng, J. Appl. Phys. **69**, 5962 (1991); SU(N) VBC have been introduced by N. Read and S. Sachdev, Phys. Rev. B **42**, 4568 (1990).
[14] A. V. Syromyatnikov and S. V. Maleyev, Phys. Rev. B **66**, 132408 (2002).
[15] P. Nikolic and T. Senthil, Phys. Rev. B **68**, 214415 (2003).
[16] R. Budnik and A. Auerbach, Phys. Rev. Lett. **93**, 187205 (2004).
[17] R. R. P. Singh and D. A. Huse, Phys. Rev. B **76**, 180407(R) (2007).
[18] G. Misguich and P. Sindzingre, J. Phys.: Condens. Matter **19**, 145202 (2007).
[19] D. Schwandt, M. Mambrini, and D. Poilblanc, arXiv:1002.0774 (to be published). The weights of higher-order resonances (involving two or more hexagons) decay rapidly with $\mathcal{L}$.
[20] D. S. Rokhsar and S. A. Kivelson, Phys. Rev. Lett. **61**, 2376 (1988).
[21] C. Zeng and V. Elser, Phys. Rev. B **51**, 8318 (1995).
[22] M. Mambrini and F. Mila, Eur. Phys. J. B **17**, 651 (2000).
[23] For the frustrated QHAF on the square lattice see M. Mambrini, A. Läuchli, D. Poilblanc, and F. Mila, Phys. Rev. B **74**, 144422 (2006).
[24] B. Sutherland, Phys. Rev. B **37**, 3786 (1988); N. Read and B. Chakraborty, *ibid.* **40**, 7133 (1989).
[25] For the same procedure on the frustrated QHAF on the square lattice see A. Ralko, M. Mambrini, and D. Poilblanc, Phys. Rev. B **80**, 184427 (2009).
[26] For example, the IR of momenta K_Γ ($r_3=r_2=+$), K_B ($r_3=+$), and K_A ($r_2=+$) in TS* (Ref. 27) of the 108-site cluster ($\sigma=\pm$) contain 79 548 096, 159 073 536, and 238 642 176 fully symmetrized states, respectively. Other momenta (with larger Hilbert spaces) should not be involved in the GS manifold (see Table I).
[27] Studied dimer liquids and VBC belong to a TS named as TS*. "Other TS" refers to the three other (degenerate) TS.
[28] G. Misguich, D. Serban, and V. Pasquier, Phys. Rev. Lett. **89**, 137202 (2002).
[29] R. Moessner and S. L. Sondhi, Phys. Rev. Lett. **86**, 1881 (2001).
[30] A. Ralko, M. Ferrero, F. Becca, D. Ivanov, and F. Mila, Phys. Rev. B **76**, 140404(R) (2007).
[31] As the fidelity, this quantity is a useful tool to identify quantum phase transitions. See S. Chen, L. Wang, Y. Hao, and Y. Wang, Phys. Rev. A **77**, 032111 (2008).
[32] Reversely, the $\mathcal{N}=48$ cell does not fit in the 108-site cluster. The $3\times4\sqrt{3}\times4\sqrt{3}$ cluster (144 sites) which can accommodate *both* $\mathcal{N}=36$ and $\mathcal{N}=48$ cells is out of reach.
[33] C. Xu and S. Sachdev, Phys. Rev. B **79**, 064405 (2009).
[34] P. Sindzingre and C. Lhuillier, EPL **88**, 27009 (2009).
[35] A. Ralko, F. Becca, and D. Poilblanc, Phys. Rev. Lett. **101**, 117204 (2008).